Plasmonic Silver – N/TiO$_2$ Effect on Photoelectrocatalytic Oxidation Reaction

Muhammad Nurdin*, Muh. Zakir Muzakkar, Maulidiyah Maulidiyah, Nurjannah Maulidiyah, Dwiprayogo Wibowo

Department of Chemistry, Faculty of Mathematics and Natural Sciences, Universitas Halu Oleo,
Kendari 93232 – Southeast Sulawesi, Indonesia

Abstract

Plasmonic effect of Ag-N/TiO$_2$ has been studied by photoelectrocatalytic oxidation reaction system. the synthesis of TiO$_2$/Ti has been carried out by anodizing method and continued by doping of nitrogen (N) and silver (Ag). The doping of N at the TiO$_2$/Ti electrode was applied by dip-coating method using NH$_4$Cl as the source of N, while the doping of Ag at N-TiO$_2$/Ti electrode was applied by electrodeposition method using AgNO$_3$ as the source. SEM characterization result indicated the form of the tube at the TiO$_2$ structure, XRD result showed the crystal anatase structure of TiO$_2$, FTIR showed the N-O functional groups at wavenumber of 1267 cm^{-1}, as the evidence of N attachment at the N-TiO$_2$ structure, EDX confirm about N and Ag of Ag-N/TiO$_2$ electrode, with however Ag percentage was 4.9%. The activity test of Ag-N/TiO$_2$ electrode by Linear Sweep Voltammetry (LSV) showed the electrode activities on the visible light, the TiO$_2$/Ti electrode has activities on the UV light. Then, the TiO$_2$/Ti and Ag-N/TiO$_2$ electrodes were tested by using Multi Pulse Amperometry (MPA) followed by using UV-Vis spectrophotometer for the degradation test of Rhodamine B (RhB) compound. The degradation test under visible light of Ag-N/TiO$_2$ electrode has good performance for 1 ppm as much as 44.2%.

Keywords: Photoelectrocatalysis, Electrode, TiO$_2$/Ti, Ag-N/TiO$_2$, Anodizing, Rhodamine B

1. Introduction

Textile industry is an industry that provides quite vast contribution towards the national economic growth [1]. The productions of textile industry such as textile materials undergo several stages of processing which likely produce waste in the form of solid, liquid, or gas waste. Liquid waste of textile industry originates from dyeing and washing process. This waste is classified as organic waste which is non-biodegradable; it is usually formed by azo compounds and benzene-derived compounds [2, 3]. Benzene group is very difficult to be degraded, that it takes a long time to be degraded and this compound can be very harmful to the environment because its carcinogenic attribute. RhB is synthetic coloring substance of azo compound in the form of greenish or purplish-red crystal powder which is soluble in high concentration and in the form of red crystal powder which is soluble in low concentration [4, 5]. This compound is commonly used in dying process to produce red color. The waste of RhB during dying process is very hazardous when it exposes aquatic environment due to its carcinogenic and undegradable qualities [6].

Many kinds of method have been implemented to overcome problems caused by azo compound; one of the methods is photocatalysis which combines photochemical and catalytic processes [7, 8]. This method plays an important role in reducing poisonous-organic substances by using UV light in order to create oxidizing and reducing species in the surface of catalyst [9]. Generally, the use of photocatalyst degrades organic pollutant perfectly into carbon dioxide in water. TiO$_2$ semiconductor is frequently used as photocatalysis substance because

it is non-toxic, stable chemically and in physics, resistant to corrosion and relatively affordable [10-13]. Based on those basic traits of TiO_2, it is continuously developed to overcome environmental problems; however, the large band gap of TiO_2 anatase crystal (approximately 3.2 eV) which is equal to UV light (388 nm wavelength) causes photocatalyst application which is restricted only within UV area [14, 15]. It is widely known that visible light comes from sunlight which supply is abundant and very beneficial when it uses photocatalyst of sunlight [16].

One technique believed effective to decrease the band gap of TiO_2 is doping technique carried out by attaching dopant to the matrix of TiO_2 crystal in which dopant element creates new catalyst matrix that has smaller band gap equal to the energy of visible light [17]. A high-quality dopant has been vastly examined by attaching nitrogen (N) because the size of N is not too different to oxygen (O) and its ionization energy is small that it can reduce the band gap of TiO_2 [18-20]. The synthesis of nitrogen doped TiO_2 (N-TiO_2) nanocrystalline is carried out by using sol-gel method; it is done by Maulidiyah et al. with titanium tetraisopropoxide (TTIP) as the precursor [21]. Maulidiyah et al. has also synthesized N-TiO_2 photocatalyst by using the same method in order to degrade congo red photocatalytically in the area of visible light [22].

Another research reported that TiO_2 nanotube which is attached or decorated by Au, Ag, and Pt provides better photocatalytic activity because of plasmonic effect within the area of visible light [23-25]. Of those three transitional modifying elements, Ag is affordable and able to provide better remediation of performance [21]. Thus, Albiter et al. has carried out research on doped N-TiO_2 nanotube preparation decorated by transitional metal (Ag) to obtain plasmonic activity within the area of visible light [26]. The use of photocatalyst in water refinement or waste processing contends with several problems including its relatively low efficiency [11]. Researchers attempt to manage this problem by combining photocatalysis with electrochemical process; this combination is widely known as photoelectrocatalysis [27-30]. The effectiveness of oxidation can be improved by applying potential bias to surge electrons through external circuit that prevents recombination of positive hole and electron; this is the principle of photoelectrocatalysis [31-34]. In this research, plasmonic effect of Ag-N/TiO_2 electrode analysis was carried out to increase organic pollutant degrading capability in water and under visible light. This system examines the efficiency of photoelectrocatalysis principle in degrading organic RhB.

2. **Experimental**

2.1 *Preparing of Titanium Plate*
The preparation of titanium plate was managed by cutting Ti plate (Shanxi Yuanlian Rare Metal Ltd, China) with 99.9% of refinement rate by the size of 4 cm x 0.5 cm and thickness of 0.5 mm. Then, the plate which has been already cut was made cleaner and spotless by stroking 1200 cc sandpaper to its surface. It was then soaked with the mixture of solutions consisting of HF, HNO_3 and distilled water with the ratio of 1 mL : 3 mL : 6 mL for 2 minutes. The last step of this preparation is rinsing Ti plates with distilled water in order to remove etching in its surface and putting it aside to dry [21, 31].

2.2 *Producing TiO₂/Ti layer by implementing Anodizing Method*
Titanium plate which had been prepared was inserted into probe filled with electrolyte solution of NH_4F 0.27 M in 98% of glycerol. Anodizing process was managed by placing Ti plate as anode and Cu plate as cathode and setting up 25 volt of electricity potential changes and this process was carried out for 4 hours. The last step managed is heating up Ti plate for 1.5 hours at the temperature of 500°C in order to obtain the crystalline of TiO_2 anatase [21, 31].

2.3 *Doping Nitrogen (N) in TiO₂/Ti Electrode*
TiO_2 and N-TiO_2 preparation method is conducted by making solution 1 containing colloid solution of TiO_2 that is 4 mL of TTIP, 0.5 mL of Acetyl Acetonate (AcAc), and 15 mL of ethanol 99% and solution 2 containing 15 mL of ethanol 99% and 2 mL of distilled water with the addition of 1 mL of acetate acid 0.1 M. Those two solutions were mixed and refluxed for 3 hours at the temperature of 50°C. The 2 mL of NH_4Cl 5 M was added to TiO_2 sol which was formed; it was stirred using magnetic stirrer for an hour at the temperature of 50°C to produce TiO_2 sol containing nitrogen (N-TiO_2). TiO_2/Ti plate was successfully synthesized before being dip coated and furnace at the temperature of 150°C for 15 minutes [21].

2.4. *Doping Silver (Ag) in N-TiO$_2$/Ti Electrode*

During electrodeposition process, N-TiO$_2$/Ti electrode was managed by using AgNO$_3$ solution with 0.04 g of electrolyte solution concentration dissolved in 100 mL of distilled water. EDTA (0.5 g) was added to 100 mL of distilled water. Those two solutions were mixed up. Electrodeposition method was conducted for 5 seconds with the potential electricity of 1.0 volt; titanium plate with N-TiO$_2$ in it was used as cathode and copper plate was used as anode. Ag-N/TiO$_2$ electrode which was formed was stored in desiccator for 24 hours [21].

3. **Results and discussion**

3.1. *Preparing Titanium (Ti) Plate*

The preparation of titanium plate was managed by cutting Ti plate with 99.9% of refinement rate by the size of 4 cm x 0.5 cm and thickness of 0.5 mm. Then, the plate which has been already cut was made cleaner and spotless by stroking 1200 cc sandpaper to its surface. It was then soaked with the mixture of solutions consisting of HF, HNO$_3$ and distilled water with the ratio of 1 mL : 3 mL : 6 mL for 2 minutes [21]. HF solution was needed to reduce and dissolve oxide layer which might still attach on the surface of the plate. HNO$_3$ solution oxidizes and removes fat or debris of the plate surface. The last step of this preparation is rinsing Ti plates with distilled water in order to remove etching solution on its surface and putting it aside to dry. From the result, it can be clearly seen that Ti plate is clean and shining which means that Ti plate is ready to cultivate TiO$_2$ on the surface by implementing anodization method. Figure 1 shows the difference of titanium plate before and after preparation.

Figure 1: Titanium surface; (a) before preparation; (b) after preparation.

3.2. *Producing TiO$_2$/Ti electrode*

Thin layer of TiO$_2$/Ti on the surface of titanium was produced by using anodizing method (Figure 2) which was conducted for 4 hours using potential bias of 25 volt and electrolyte solution of NH$_4$F 0.5% in glycerol. Higher voltage was supplied in the process of producing thin layer of TiO$_2$/Ti that makes the structure shape like nodule or particulate. Generally, anodizing process will form nanomaterial which is 1-100 nm in size [35].

Anodizing process was managed based on electrolysis process in which titanium (Ti) metal was used as anode and copper (Cu) metal was used as cathode which was connected to DC Power Supply current. Oxidation process occurred in anode forming thin layer of TiO$_2$ on the surface of titanium. Reduction reaction took place in cathode resulting hydrogen gas characterized by the formation of bubbles on the surface of Cu metal [31].

Thin layer of TiO$_2$/Ti from anodizing process was calcined at the temperature of 500°C for 1.5 hours to vapor the remaining organic solvent got trapped during anodizing process. In addition, this calcination process aimed to obtain TiO$_2$/Ti electrode with crystal anatase structure which has photoactive quality [27]. TiO$_2$ with crystal anatase structure has greater surface and greater active parts that enable it to better absorb light rather than rutile crystal. Anatase structure has 3.2 eV of band gap energy which is equal to UV wavelength which is < 388 nm [36]. This band gap energy indicates the extent to which the energy is needed to manage electron transition from valence band to conduction band. TiO$_2$/Ti electrode from calcinations is exhibited in Figure 2.
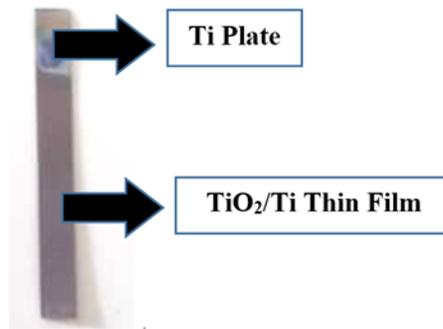
Figure 2: The Surface of TiO_2/Ti Electrode.

The surface of titanium which had been cultivated with TiO_2 nanotube from anodization process turned grayish and the surface turned smooth, while the segregated part turned blue due to calcinations process [37].

3.3. *Producing Ag-N-TiO₂/Ti Electrode*

Nitrogen was attached to TiO_2 structure in order to increase the activity of TiO_2 in degrading organic substance under visible light. The addition of N produced orbital with new position (originating from the orbital of 2p N) between valence band (consists of 2p O) and conduction band (consist of 3d Ti). Orbital 2p of N stands as the step up for electron in orbital 2p of O; thus, it only requires low energy to make the electron experience excitation (stepping electron) from valence band to conduction band [38, 39].

Doping N on the surface of TiO_2/Ti was conducted using sol-gel method. This method has several advantages including the conditions of reaction which are easily controlled such as its pH, temperature, and hydrolysis rate [40]. Sol-gel production was managed by using TTIP solution as the precursor, AcAc as chelating ligand which produces exothermic reaction and turns into yellow solution, ethanol as organic solvent, acetate acid which control pH of the solution, and destilled water which hydrolyzes TTIP into $Ti(OH)_4$ and then experiences condensation reaction forming long chains which intertwines and forms gel and NH_4Cl 5 M as the source of N. The attachment process of N to TiO_2 was managed using dip coating; dipping TiO_2/Ti plate into sol-gel of $N-TiO_2$ to form transparent layer on the surface of TiO_2/Ti which was followed by heating it up at the temperature of 150°C in order to produce $N-TiO_2$/Ti electrode.

Ag coating to the surface of $N-TiO_2$ aimed to decrease the value of band gap and prevent the recombination of electron on the surface in which electron in conduction band is trapped by Ag metal that the electron could not undergo electron recombination (back to its initial condition) [21]. Thus, the hole of valence band will always be active in degrading organic substance of water. $Ag-N/TiO_2$ electrode from the synthesis is exhibited in Figure 3.
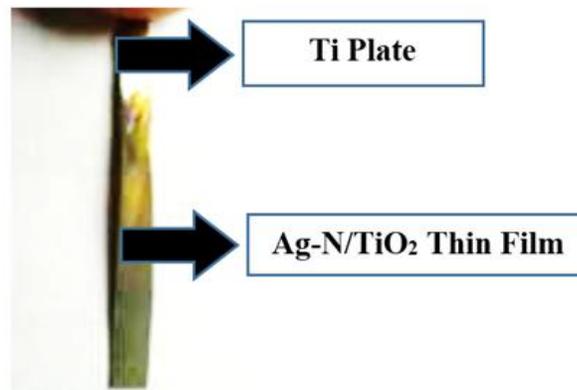

Figure 3: The Surface of $Ag-N-TiO_2$/Ti Electrode.

Doping Ag on the surface of N-TiO$_2$/Ti using electrodeposition method was managed based on the process of breaking down an electrolyte which was electrified using two polarized electrodes, hence metal deposition process occurred electrochemically. This method of deposition requires one-way electric current thus Cu metal was used as anode and N-TiO$_2$/Ti plate was used as anode. In this system, cation moves to cathode and anion moves to anode. Electrolyte solution used is AgNO$_3$ 0.1% in EDTA solution. EDTA solution functions to chelate Ag ion which is expected to make the distribution of Ag run regularly. Electrodeposition was conducted for 5 seconds and within 0.5 volt of potential bias; this was conducted rapidly to produce very thin layer of Ag and enable the production of pores that light coming can penetrate Ag layer and cause excitation of electron on the surface of N-TiO$_2$/Ti. Therefore, hole will be active even longer in degrading organic substances.

3.4. *Characterization of Work Electrode*
3.4.1. *Determination of TiO$_2$ Crystal Anatase Structure using X-Ray Diffraction (XRD)*
The analysis of TiO$_2$/Ti electrode using XRD aimed to identify crystal structure of TiO$_2$/Ti formed by the synthesis process. The characterizations results of TiO$_2$/Ti electrode reveal the existence of TiO$_2$ crystal anatase reported found by Nurdin and Maulidiyah using the same method. Diffractogram of TiO$_2$ anatase [31] is exhibited in Figure 4.
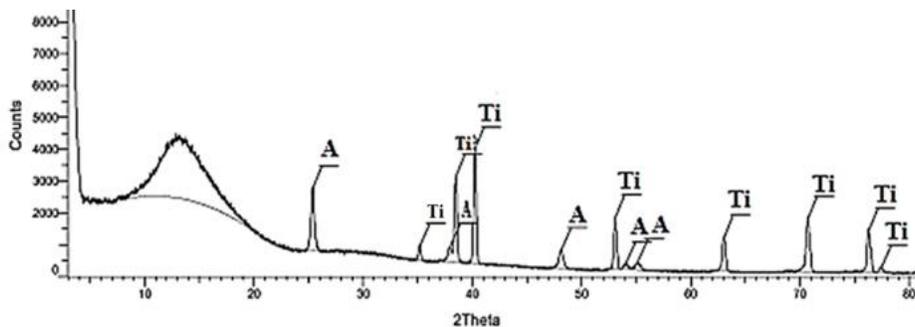

Figure 4: Diffractogram of TiO$_2$ anatase on the surface of Ti plate.

Based on the results of XRD pattern of the thin layer of TiO$_2$/Ti exhibited in Figure 4, it can be seen that crystal phase in the form of anatase is characterized by the formation of particular peaks with anatase structure.

3.4.2. *Characterization Using Scanning Electron Microscopy (SEM)*
The preparation of thin film TiO$_2$/Ti using the anodizing method to obtain TiO$_2$ nanotube with the tube size of 10-60 nm [31]. It explained the appearance of pores and void spaces on the surface of TiO$_2$ for the formation of the nanotube and the high acidity to helps the pores form. This technique will result in TiO$_2$/Ti formation on the surface of Ti plate [21].

3.4.3. *Characterization of Fourier Transform Infrared Spectroscopy (FTIR)*
Based on the results of characterization using FTIR, N-TiO$_2$ spectrum was obtained; this spectrum is exhibited in Figure 5.

The indication of O-H group is identified by the emergence of wavenumber within the uptake of 3210 cm^{-1}. OH group originates from Ti-OH, water, and ethanol with very strong signal. The indication of O-Ti-O group lies in the wavenumber of 811 cm^{-1} and N-O group lies in 1267 cm^{-1} uptake [41]. The uptake indicating –N-O group becomes the signal of successful attachment of nitrogen in the structure of TiO$_2$.

3.4.4. *Characterization Using EDX*
The results of EDX characterization reveal morphological form of Ag-N/TiO$_2$ and the positions of N and Ag within Ag-N/TiO$_2$ electrode as exhibited in Figure 6.
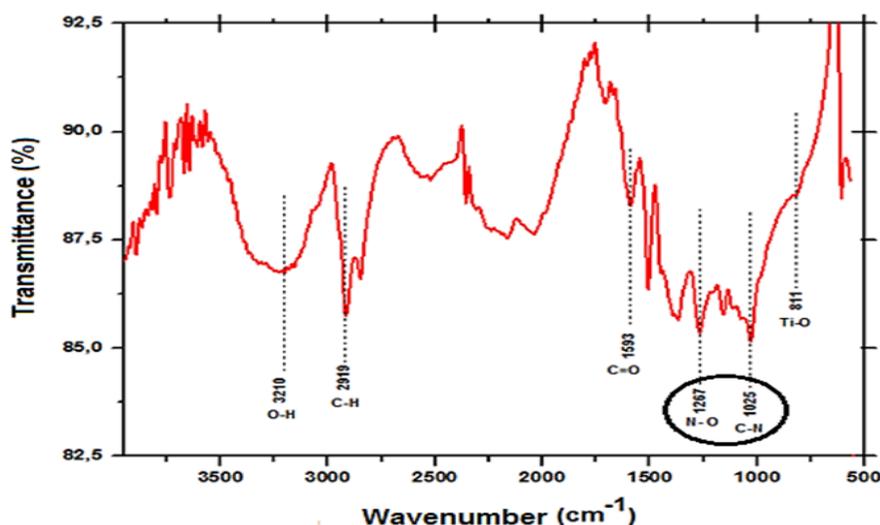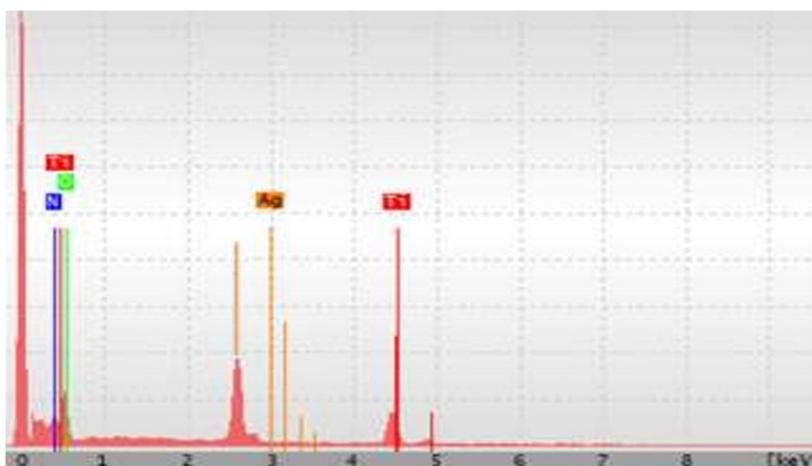
Figure 5: FTIR Spectrum of N-TiO$_2$.

Figure 6: EDX Characterization Results of Ag- N/TiO$_2$

Figure 6 depicts EDX data from Ag-N/TiO$_2$ electrode from the synthesis. The successful attachment of N and Ag is characterized by the emergence of peak within the rate of energy of 0.392 keV indicating the existence of N, while the existence of Ag is characterized by the emergence of equally distributed peak within three levels of energy, i.e. 2.644 keV, 2.984 keV, 3.151 keV, and 3.520 keV. The EDX spectrum of Ag nanoparticles demonstrates the distinct presence of Ag peaks at 2.984 KeV, 3.151 keV, 3.348 keV, 3.52 keV and 2.644 keV [42]. The amount of nitrogen in Ag-N/TiO$_2$ electrode reaches 10.8%, while the amount of Ag reaches 4.9%. The addition of Nitrogen to TiO$_2$ can increase absorbent ranging from 400 nm – 700 nm.

3.4.5. *Characterization Using Linear Sweep Voltammetry (LSV)*
The measurement of light current as potential function using LSV technique was managed by using electrolyte solution of NaNO$_3$ 0.1 M connected to Portable Pontensiostat. The measurement using LSV utilizes three electrodes, i.e. TiO$_2$/Ti and Ag-N/TiO$_2$ electrodes as operational electrode, platinum (Pt) as counter electrode, and Ag/AgCl as comparative electrode. Operational electrodes of TiO$_2$/Ti and Ag-N/TiO$_2$ were measured alternately to compare the activities of both electrodes when they are ignited using UV and visible light during photoelectrocatalysis process.
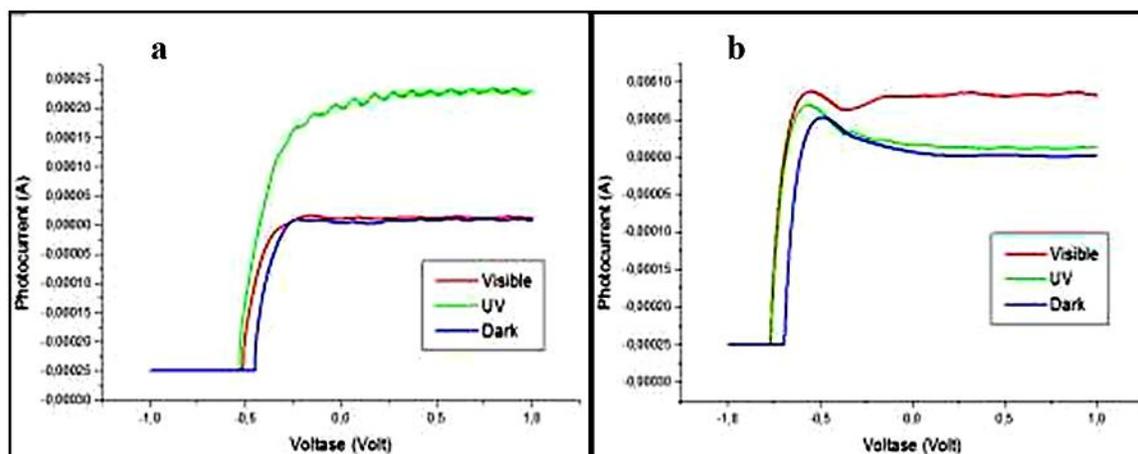
Figure 7: Test of Electrode Activity using Linear Sweep Voltammetry (LSV): (a) TiO_2/Ti electrode, (b) Ag-N/TiO_2 electrode

Figure 7.a shows that TiO_2/Ti electrode under UV light exposure has better activity than electrode under visible light; it is because TiO_2/Ti electrode with crystal anatase structure is only active under UV light with 365 nm – 388 nm wavelength. In the darkness, there was no light-related response in TiO_2/Ti electrode during measurement because, in the darkenss, TiO_2/Ti electrode could not produce energy which would be transmitted from valence band to conduction band.

Figure 7.b shows that the plasmonic effect of Ag-N/TiO_2 electrode under visible light has better activity than under UV light; this is in line with the study of Maulidiyah et al. that the addition of N and metal substance can increase the performance of electrode in visible area and decrease the performance in UV area [21]. The addition of N and Ag can move the conduction band and lessen the value of band gap. Therefore, Ag-N/TiO_2 electrode can absorb light which wavelength is greater with lower energy.

3.4.6. *Degradation Test of Rhodamine B using TiO_2/Ti and Ag-N-TiO_2/Ti Electrodes*
Performance test of TiO_2/Ti and plasmonic effect of Ag-N/TiO_2 electrodes was implemented using RhB. The maximum wavelength of RhB obtained from the result of measurement using spectrophotometer UV-Vis is 552 nm as depicted in Figure 8.
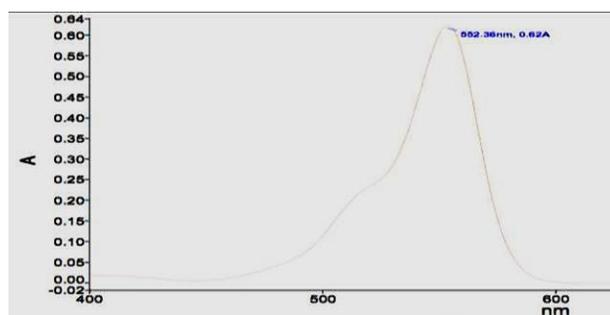

Figure 8: Maximum Wavelength of RhB

During the measurement process, electron transition took place; it involved π electrons which ere conjugated along the chromophore group of heterocyclic RhB by absorbing energy and this substance is read because of transition in the area of visible light [21]. Based on the result of measurement of each standardized solution, it formed calibration curve with linear equation of $y = 0.204x + 0.017$.

Degradation test of organic RhB using photoelectrocatalysis process with potensiostat tool (MPA) and Spectroscopy UV-Vis was carried out to identify the decreased concentration of each solution. Degradation process was conducted using photolysis; a process of breaking a substance down using only radiation light.

Photocatalysis is a process of breaking organic substance down by utilizing light and catalyst. Photoelectrocatalysis is the combination of photocatalysis and electrochemical process which brings light, catalyst, and electron into play.

The absorption of UV light by TiO_2/Ti catalyst produces hole (h^+) which then creates •OH when it responds to water. •OH plays an important role in breaking the structure of organic substance. Degradation process of organic RhB is exhibited in Figures 9 and 10. The peaks of RhB degradation absorbances data obtained have been calculated in to concentration.
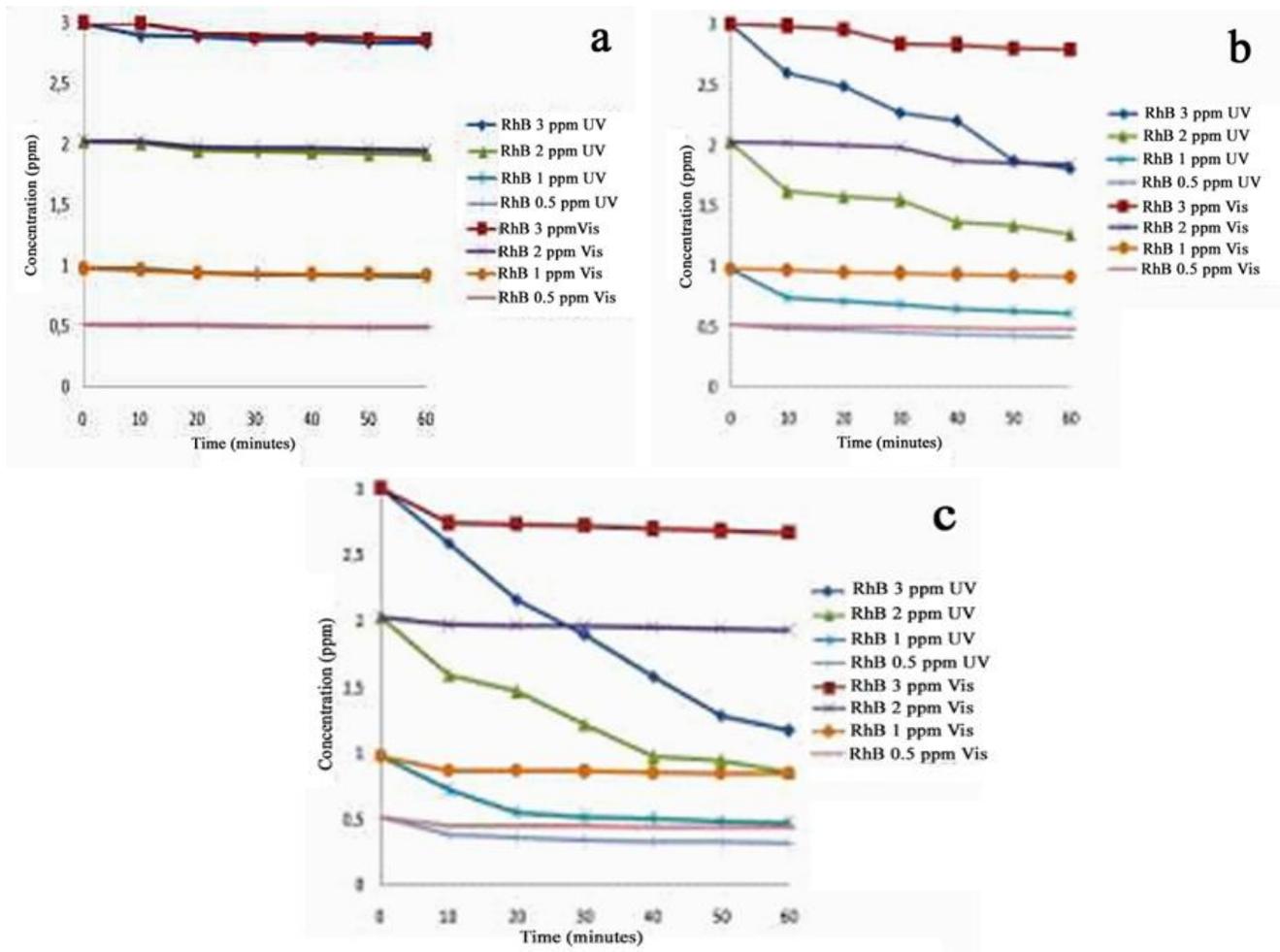

Figure 9: Degradation of RhB by TiO_2/Ti electrode using, (a) photolysis process; (b) photocatalysis process; (c) photoelectrocatalysis process

Degradation process of RhB using photocatalysis process indicates that the concentration of RhB decreases very slowly when it is radiated either by UV and visible light as depicted in Figure 9.a. However, TiO_2/Ti catalyst increases the degradation under UV light (Figure 9.b); it means that TiO_2/Ti electrode with better activity under UV light has been successfully produced; it is supported by LSV data (Figure 9.a). The addition of electron (electric current) prevents recombination of electron-hole during light illumination that the degradation process occurs more rapidly (Figure 9.c). Degradation using photoelectrocatalysis process has greater rate of degradation than those of photolysis and photocatalysis process. N and Ag in TiO_2/Ti catalyst can increase the performance of Ag-N/TiO_2 electrode within the area of visible light as exhibited in Figure 10.
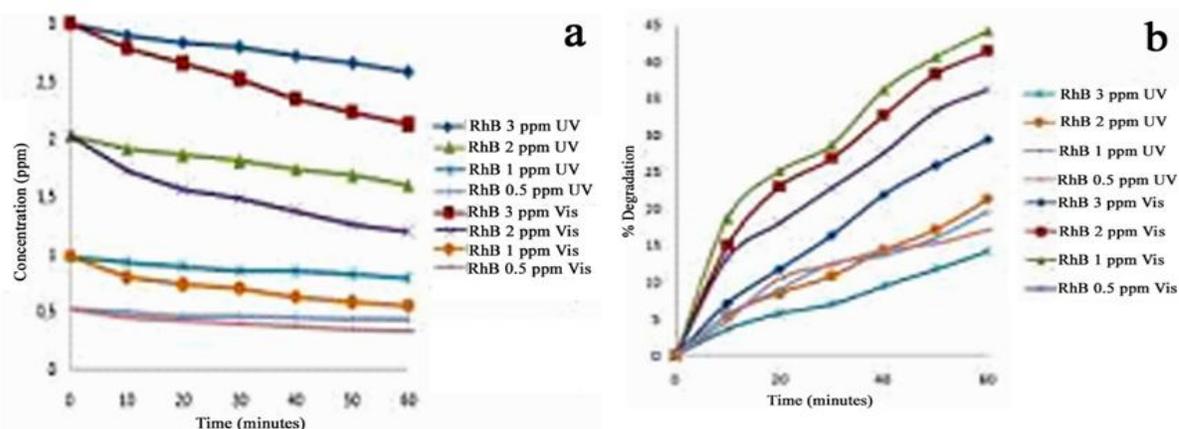
Figure 10: (a) Degradation Data of RhB; (b) the percentage % of degradation by Ag-N/TiO$_2$ electrode using photoelectrocatalysis

Based on Figure 10, it can be stated that the performance of Ag-N/TiO$_2$ electrode in degrading RhB under visible light is better than under UV light. This is in line with the research conducted by Kang et al. that N-TiO$_2$ which is decorated with metals such as Pt, Cu, Cr, and Fe which can increase N-TiO$_2$ in degrading Congo Red substance [43]. Nitrogen and Silver on the surface of TiO$_2$ from the synthesis can narrow the gap energy of TiO$_2$ so that it requires lower energy for the electron to experience excitation from valence band to conduction band. Therefore, •OH which is formed in photocatalystic process will be merrier and, consequently, degradation process will run rapidly. Maximum degradation energy of Ag-N/TiO$_2$ electrode towards organic RhB under visible light is exhibited in Figure 10.b. The value of maximum degradation is obtained from RhB by the concentration of 1 ppm as much as 44.2%.

Conclusions
1. Plasmonic effect of Ag-N/TiO$_2$ electrode has better activity when it is exposed by visible light than UV light because the attachment of N and Ag can decrease gap energy that the energy required for electron to experience excitation from valence band to conduction band becomes less. TiO$_2$/Ti has higher activity during the exposure of UV light during photoelectrocatalysis process than of visible light.
2. Ag-N/TiO$_2$ electrode has higher performance in degrading RhB under visible light within photoelectrocatalysis process with the percentage of maximum degradation of 44.2%. While the performance of TiO$_2$/Ti electrode is faster in degrading RhB when it is exposed by UV light during photoelectrocatalysis process.

References
1. Rahman M.H., Siddiqui S.A. *Inter. J. Sci. & Res. Pub.* 5 (2015) 1.
2. Lai C.W., Juan J.C., Ko W.B., Hamid S.B.A. *Inter. J. Photoenergy*, 2014 (2014) 1.
3. Varshney G., Kanel S.R., Kempisty D.M., Varshney V., Agrawal A., Sahle-Demessie E., Varma R.S., Nadagouda M.N. *Coordination Chem. Rev.* 306 (2016) 43.
4. Barka N., Qourzal S., Assabbane A., Nounah A., Ait-Ichou Y. *J. Photochem. & Photobio. A: Chem.* 195 (2008) 346.
5. Moutusi D., Bhattacharyya K.G. *J. Mol. Cat. A: Chem.* 391 (2014) 121.
6. Carneiro J.O., Samantilleke A.P., Parpot P., Fernandes F., Pastor M., Correia A., Luis E.A., Barros A.A.C., Teixeira V. *J. Nanomaterials* 2016 (2016) 1.
7. Maulidiyah, Ritonga H., Salamba R., Wibowo D., Nurdin M. *Inter. J. ChemTech Res.* 8 (2015) 645.

8. Li Z-D., Wang H-L., Wei X-N., Liu X-Y., Yang Y-F., Jiang W-F. *J. Alloys and Compounds* 659 (2016) 240.
9. Anas M., Han D.S., mahmoud K., Park H., Abdel-Wahab A. *Mater. Sci. Semicon. Proc.* 41 (2016) 209.
10. Fang Y., Sun M., Wang Y., Sun S., He J. *Mater. Res. Bulletin* 74 (2016) 265.
11. Liu Y., Quan B., Ji G., Zhang H. *Mater. Let.* 162 (2016) 138.
12. Pal N.K., Kryschi C. *Chemosphere* 144 (2016) 1655.
13. Nurdin M., Maulidiyah, Watoni A.H., Abdillah N., Wibowo D. *Int. J. ChemTech Res.* 9 (2016) 483.
14. Hashimoto K., Irie H., Fujishima A. *Japanese J. App. Phy.* 44 (2005) 4.
15. Maulidiyah, Wibowo D., Hikmawati, Salamba R., Nurdin M. *Orient. J. Chem.* 31 (2015) 2337.
16. Maulidiyah, Ritonga H., Faiqoh C.E., Wibowo D., Nurdin M. *Biosci. Biotech. Res. Asia* 12 (2015) 1985.
17. Liu C., Zhang L., Liu R., Gao Z., Yang X., Tu Z., Yang F., Ye Z., Cui L., Xu C., Li Y. *J. Alloys & Comp.* 656 (2016) 24.
18. Tang Y-C., Huang X-H., Yu H-Q., Tang L-H. *Inter. J. Photoenergy* 2012 (2012) 1.
19. Viswananthan B., Krishanmurthy K.R. *Inter. J. Photoenergy* 2012 (2012) 1.
20. Hamadanian M., Karimzadeh S., Jabbari V., Villagran D. *Mater. Sci. Semicon. Proc.* 41 (2016) 168.
21. Maulidiyah, Nurdin M., Wibowo D., Sani A. *Inter. J. Pharma. Pharma. Sci.* 7 (2015) 141.
22. Maulidiyah, Nurdin M., Widianingsih E., Azis T., Wibowo D. *ARPN J. Engin. & Appl. Sci.* 10 (2015) 6250.
23. Wang Q., Wang X., Zhang M., Li G., Gao S., Li M., Zhang Y. *J. Coll. & Interface Sci.*, 463 (2016) 308.
24. Hou L., Li S., Lin Y., Wang D., Xie T. *J. Coll. & Interface Sci.*, 464 (2016) 96.
25. Shuang, Shuang Lv., Xie R., Zhang Z., Zhengjun. *Nature (Scientific Reports)* 6 (2016) 26670.
26. Albiter E., Valenzuela M.A., Alfaro S., Valverde-Aguilar G., Martinez-Pallares F.M. *J. Saudi Chem. Soc.* 19 (2015) 563.
27. Nurdin M., Wibowo W., Supriyono, Febrian M.B., Surahman H., Krosnandi Y.K., Gunlazuardi J. *MAKARA, SAINS*, 13 (2009) 1.
28. Nurdin M. *Inter. J. Pharma & Bio Sci.* 5 (2014) 360.
29. Maulidiyah, Nurdin M., Erasmus, Wibowo D., Natsir M., Ritonga H., Watoni A.H. *Inter. J. ChemTech Res.* 8 (2015) 416.
30. Zhang Z., Chang X., Chen A. *Sensors and Actuators B* 223 (2016) 664.
31. Nurdin M., Maulidiyah. *Inter. J. Sci. & Tech. Res.* 3 (2014) 122.
32. Hua Z., Dai X., Bai X., Ye Z., Wang H., Gu H., Huang X. *Chem. Engin. J.* 283 (2016) 514.
33. Zhou X., Zhang X., Feng X., Zhou J., Zhou S. *Dyes & Pigments* 125 (2016) 375.
34. Bessegato G.G., Cardoso J.C., Silva B.F.d, Zanoni M.V.B. *Appl. Catal. B: Environ.* 180 (2016) 161.
35. Ratnawati, Gunlazuardi J., Dewi E.L., Slamet. *Inter. J. Hydrogen Energy*, 39 (2014) 16927.
36. Chen X., Wei J., Hou R., Liang Y., Xie Z., Zhu Y., Zhang, Wang H. *Appl. Catal. B: Environ.* 188 (2016) 342.
37. Juang Y., Liu Y., Nurhayari E., Thuy N.T., Huang C., Hu C-C. *Chemosphere,* 144 (2016) 2462.
38. Asahi R., Morikawa T., Ohwaki T., Aoki K., Taga Y. *Science.* 293 (2001) 269.
39. Wawrzyniak B., Morawski A.W., Tryba B. *Inter. J. Photoenergy*, 2006 (2006) 1.
40. Owens G.J., Singh R.K., Foroutan F., Aqaysi M., Han C-M., Mahapatra C., Kim H-W., Knowles J.C. *Progress in Mater. Sci.* 77 (2016) 1.
41. Ruslan, Wahab A.W., Nafie N.L., Nurdin M. *Inter. J. Sci. & Tech. Res.*, 2 (2013) 220.
42. Tien D-C., Chen L-C., Thai NV., Ashraf S. *J. Nanomater. (Hindawi Pub. Corp.),* 2010 (2010) 1.
43. Kang Y-G., Lee K-H., Hahm H-S. *Turkish J. Chem.*, 39 (2015) 159.

(2016); <http://www.jmaterenvironsci.com/>